

Development of Gold-Alloy Nanocomposite for Tetrahydrocurcumin Delivery

Lim Chiou Chyi¹, Tan Kin Fai¹, Shiau-Chuen Cheah², and Palanirajan Vijayaraj Kumar^{1*}

¹Department of Pharmaceutical Technology, Faculty of Pharmaceutical Sciences, UCSI University, Kuala Lumpur 56000, Malaysia

²Faculty of Medicine and Health Sciences, UCSI University, Taman Connaught, Cheras, 56000, Kuala Lumpur, Malaysia

*Corresponding author. vijayarajkumar_p@yahoo.com

Abstract

The phytochemical tetrahydrocurcumin (THC), a major metabolite of curcumin, demonstrates higher anticancer activity, systemic bioavailability, and stability than curcumin itself. However, the poor aqueous solubility of THC causes it to be susceptible to oxygen and is poorly absorbed in the gastrointestinal tract. Therefore, a delivery system is needed to address the delivery issues of THC. Gold-copper nanocomposites (Au-CuNPs) are good candidates for drug delivery and have been shown to have anticancer and antibacterial effects with the advantages of decreasing the cost of gold and enhancing the stability of copper. In this study, a nanocomposite composed of gold and copper alloy was used to design a THC delivery system.

The Turkevich method was used to create a bioengineered Au-CuNP system for delivering the herbal phytochemical THC. UV spectroscopy, FTIR analysis, drug entrapment efficiency, and zeta potential were used to characterise the prepared bioengineered nanocomposite system. To confirm the biological properties, xCELLigence real-time monitoring of the Caco-2 cell cytotoxic activity of THC-loaded gold-copper nanocomposites (THC Au-CuNPs) was performed.

Au-CuNPs in a 1:1 ratio was selected to prepare the THC delivery system. The amount of THC loaded was optimised by selecting 2 mg THC due to the highest

possible amount of drug loading with optimum nanoparticle size characteristics. FTIR analysis showed that THC was successfully loaded in the delivery system. The mean particle diameter of THC Au-CuNPs was 248.8 nm, indicating the successful formation of nanocomposites. The cell culture studies showed that the THC Au-CuNPs have significant cytotoxic activity on Caco-2 cell lines.

Finally, the anticancer activity of the THC Au-CuNPs was confirmed in this study.

Keywords: Gold Nanoparticle, Copper Nanoparticle, Tetrahydrocurcumin, Nanocomposite

Introduction

Cancer is a primary cause of mortality and a significant obstacle to extending life expectancy in every country (1,2); thus, it is one of the major public health concerns worldwide. Generally, colorectal cancer ranks third as the most commonly diagnosed cancer but second as the major cause of cancer-related death. There was one colorectal cancer case among 10 cancer cases and deaths (2).

Phytochemicals are natural substances originating from plants with medicinal actions against a variety of human diseases (3). Curcumin is one of the active compounds naturally occurring in turmeric, which is the rhizome of the herb *Curcuma longa* (4). It has preventive and therapeutic effects on cancers due to its anticancer mechanism (5,6). Nevertheless, curcumin degrades rapidly at

physiological pH (7.4), and in the presence of light, it also has low stability in aqueous solutions (7-9). Because of its chemical instability and poor pharmacokinetics, curcumin has inferior systemic bioavailability (10).

Tetrahydrocurcumin (THC), a major colorless metabolite of curcumin, shows better activity than curcumin in the treatment of various cancers and has stronger antioxidant action (4,10-14). It has great stability in plasma and at physiological pH (8,11). Tetrahydrocurcumin is a polyphenol that is acquired by the hydrogenation of curcumin and is more polar than curcumin (15-17). Curcumin is converted into tetrahydrocurcumin after intestinal absorption (Figure 1) and then circulates in the blood and is subsequently delivered to the liver and kidney (15,18).

However, the poor aqueous solubility of tetrahydrocurcumin causes it to be susceptible to oxygen and is poorly absorbed in the gastrointestinal tract (13,19,20). This restricts its potential to be developed in water-based formulations (17). Therefore, a delivery system is needed to address the delivery issues of tetrahydrocurcumin. Gold nanoparticles (AuNPs) have some extraordinary properties, including small size, stability, easy synthesis, high surface area to volume ratio, and optical properties; thus, they are good candidates in chemotherapeutics and drug delivery (21-23). Copper is another great choice of material because it is extremely conductive and substantially cheaper (24). In addition, copper nanoparticles (CuNPs) have shown effective dose-dependent cytotoxic activity (25). In this study, a gold-copper nanocomposite

(Au-CuNP) delivery system is proposed to address the delivery issues of tetrahydrocurcumin and to decrease the cost of gold and enhance the stability of copper. The gold-copper nanocomposite has been reported to have a cytotoxic effect itself (26). In addition, Woźniak-Budych et al. reported that gold-copper nanocarriers can be applied in targeted cancer therapy due to their porosity and anticancer effect (27).

Material and Methods

Chemicals and Reagents

Tetrahydrocurcumin was manufactured by Sigma-Aldrich, India. Gold (III) chloride 99 % and sodium citrate tribasic dihydrate, ACS reagent >99.0 %, were manufactured by Sigma-Aldrich, USA. Copper (II) sulfate pentahydrate was manufactured by Merck KGaA, Germany. Dulbecco's Modified Eagle's Medium (DMEM), Trypsin-EDTA Solution, Foetal bovine serum, Penicillin-Streptomycin solution, and Phosphate Buffered Saline were obtained from ATCC, USA.

Preparation of gold nanoparticles (AuNPs) and gold-copper nanocomposites (Au-CuNPs)

AuNPs were prepared by mixing 0.5 mg of HAuCl_4 , 4 mL of ultrapure water, and 6 mg of sodium citrate, followed by stirring continuously for 1 hour at 105°C . Au-CuNPs were prepared by mixing CuSO_4 , 0.5 mg of HAuCl_4 , 4 mL of ultrapure water, and 6 mg of sodium citrate, followed by stirring continuously for 1 hour at 105°C . Au-CuNPs of different ratios were prepared by manipulating the amount of 1 mg/mL CuSO_4 in 0.5 mL, 1 mL, 1.5 mL, and 2 mL. AuNPs and Au-CuNPs were prepared to act as

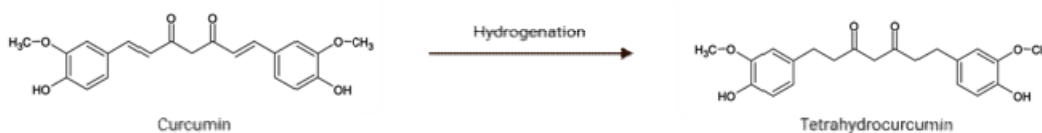


Figure 1: Transformation of curcumin into tetrahydrocurcumin by hydrogenation process

Development of Gold-Alloy Nanocomposite

controls of the tetrahydrocurcumin gold-copper nanocomposite formulation.

Preparation of tetrahydrocurcumin gold-copper nanocomposites (THC Au-CuNPs)

The preparation was based on the Turkevich method. First, 0.5 mg of CuSO_4 , 0.5 mg of HAuCl_4 , tetrahydrocurcumin, 4 mL of ultra-pure water, and 6 mg of sodium citrate were mixed together, followed by stirring continuously for 1 hour at 350 rpm at 105°C . The resulting mixture was centrifuged at 13,000 rpm for 10 minutes at 17°C . The sediments were collected and dispersed with ultrapure water until 500 μL was reached.

Surface plasmonic resonance (SPR) analysis of gold nanoparticles using UV spectroscopy

To confirm the surface plasmonic resonance of the preparation (THC Au-CuNPs) and the formation of Au-CuNPs, THC Au-CuNPs were compared with the surface plasmonic resonance (SPR) of pure AuNPs and Au-CuNPs. The preparation, pure AuNPs, and Au-CuNPs were freshly prepared and scanned under UV using a Spectrum SP-UV 500DB spectrophotometer (United Scientific, United States). Sodium citrate and ultrapure water were used as blanks. A 200 nm to 800 nm wavelength was used to perform the scan.

Fourier transform infrared (FTIR) analysis

THC Au-CuNPs, Au-CuNPs, AuNPs, and tetrahydrocurcumin were characterised by Fourier transform infrared (FTIR) analysis. All spectra were obtained by a Thermo Fisher Scientific Nicolet iS5 spectrophotometer (Thermo Fisher Scientific, United States) using OMNIC Software from 4000 to 400 cm^{-1} at a data acquisition rate of 2 cm^{-1} per point. All spectra were compared to ensure drug loading in Au-CuNPs.

Preparation of the tetrahydrocurcumin standard curve by UV spectroscopy

A stock solution of 2 mg/mL tetrahydrocurcumin was prepared by adding 20 mg of tetrahydrocurcumin powder into 10 mL of methanol. From this stock solution, 30, 40, 50, 60, and 70 $\mu\text{g/mL}$ of drugs were prepared according to the formula $M_1V_1 = M_2V_2$. These different drug concentrations were detected by a UV spectrometer (Spectrum SP-UV 500DB, United Scientific, Southern Africa) from 200 nm to 400 nm. Ethanol was used as the blank. By obtaining the absorbance at tetrahydrocurcumin lambda max, the standard curve of tetrahydrocurcumin was plotted, and the equation was obtained from the standard curve.

Detection of tetrahydrocurcumin in supernatant using UV spectroscopy

THC Au-CuNPs were freshly prepared, sonicated, transferred into Falcon tubes, and then centrifuged at 13,000 rpm for 10 minutes at 17°C . By centrifugation of the preparations, the colourless supernatant was obtained and scanned under a UV spectrometer (Spectrum SP-UV 500DB, United Scientific, United States) from 200 nm to 400 nm. The absorbance obtained at the tetrahydrocurcumin lambda max (280 nm) was multiplied by the dilution factor, and the resulting absorbance was substituted into the equation of the tetrahydrocurcumin standard curve. The total amount of tetrahydrocurcumin remaining in the supernatant was calculated. The amount of tetrahydrocurcumin entrapped in the Au-CuNPs was determined by subtracting the total amount of tetrahydrocurcumin remaining in the supernatant from the initial amount of tetrahydrocurcumin added.

Optimisation of tetrahydrocurcumin entrapment

THC Au-CuNPs were prepared with different amounts of tetrahydrocurcumin added (0.5, 1, 1.5, 2, 2.5, and 3 mg). The amount of tetrahydrocurcumin entrapped in the different concentrations of preparation was determined.

The optimised concentration for preparation of the THC Au-CuNPs would be chosen based on the nanoparticle size character and amount of drug entrapped.

Zetasizer

A Zetasizer study was performed to characterise the prepared bioengineered nanocomposite system, THC Au-CuNPs. The particle size and polydispersity index (PDI) of the preparation were determined by means of dynamic light scattering (DLS) using a Zetasizer Nano S (Malvern Panalytical, Malvern, United Kingdom).

Cell culture

To confirm the biological properties of THC Au-CuNPs, xCELLigence real-time monitoring of Caco-2 cell cytotoxic activity (28) was performed. Caco-2 (ATCC HTB-37) cells were used. It was maintained in ATCC-formulated DMEM (Dulbecco's Modified Eagle's Medium) supplemented with 10 % foetal bovine serum, 1 % penicillin/streptomycin and was incubated under a humidified atmosphere of 5 % CO₂ and 95 % air at 37°C (28).

Dynamic monitoring of cytotoxic activity using the RTCA DP system

Real-time cellular analysis (RTCA) xCELLigence technology was applied to obtain the cytotoxicity by keeping track of all cellular activities in real-time during the experiment to learn more specifically about the rate at which cells respond. Caco-2 cells were seeded in 4 wells of E-plates 16 at a concentration of 1×10^4 /well and grown for 24 hours. Then, the cells were treated with THC Au-CuNPs at the optimised tetrahydrocurcumin concentration, with Au-CuNPs acting as a blank. Readings from the xCELLigence RTCA DP instrument (ACEA Biosciences Inc., USA) were taken every 5 minutes for 24 hours and every 30 minutes for 48 hours to track the cell responses. The kinetic profile of the cellular responses and the decrease in cell index were obtained accordingly against their respective amounts.

Results and Discussion

UV spectroscopy of pure gold nanoparticles (Au-CuNPs) and gold-copper nanocomposites (Au-CuNPs)

Pure AuNPs and Au-CuNPs in different ratios were scanned from 200 nm to 800 nm to obtain their spectra (Figure 2). The lambda max of 531 nm obtained from the pure AuNPs indicated the success of the chemical reduction of HAuCl₄ to AuNPs due to the presence of surface plasmonic absorption on the gold nanoparticles (29). Figure 2 demonstrates the correlation between the formation of nanoparticles and the shift in lambda max. With the addition of copper to the AuNPs, the result showed that there is a shift in the lambda max. AuNPs are the foundation for the nonlinear optical response of the nanocomposites formed. (30) Therefore, the lambda max of the Au-CuNPs formed is derived from the lambda max of the AuNPs. Changes in the absorbance or wavelength of the surface plasmon resonance band can be used to determine the size of nanoparticles (31, 32). A redshift in the surface plasmon resonance band, which is to longer wavelengths, indicates the larger size of nanoparticles (31-33). The formation of Au-CuNPs at a ratio of 1:1 obtained a lambda max of 520 nm, indicating the smaller particle size of Au-CuNPs. On the other hand, Au-CuNPs at ratios of 1:3 and 1:4 obtained lambda max values of 546 nm and 541 nm, respectively, indicating the larger particle size of Au-CuNPs, as the shift in the surface plasmon resonance band to longer wavelengths showed the larger size of the nanoparticles (31-33). Therefore, 1:1 Au-CuNPs with the smallest particle size were chosen to load tetrahydrocurcumin.

Fourier transform infrared (FTIR) spectrometry

The presence of IR peaks at 1116 and 1076 cm⁻¹ in THC Au-CuNPs indicates that the THC is loaded in Au-CuNPs (Figure 3).

Optimisation of tetrahydrocurcumin entrapment

The lambda max of pure tetrahydrocurcumin determined by using a

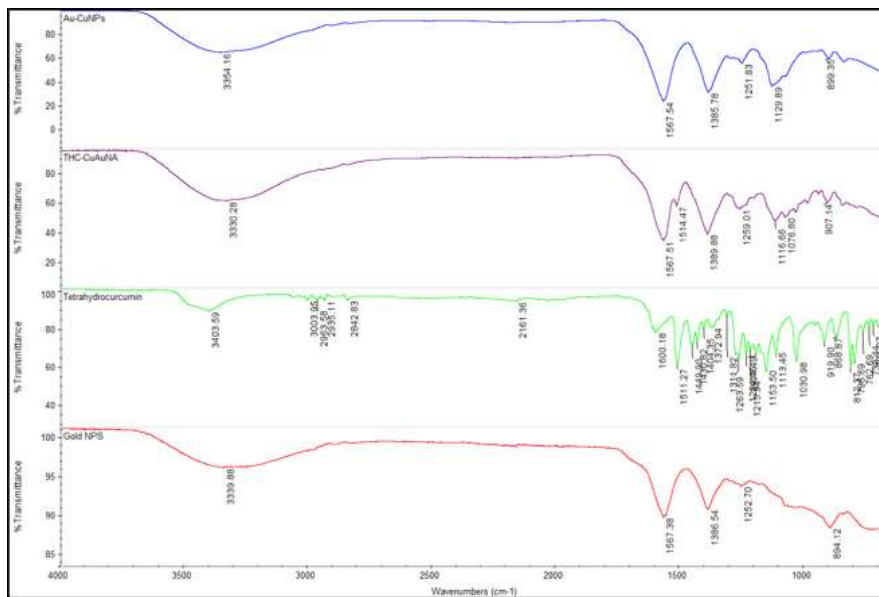


Figure 3: Infrared spectra of (a) Au-CuNPs, (b) THC Au-CuNPs, (c) tetrahydrocurcumin, and (d) AuNPs

Spectrum SP-UV 500DB spectrophotometer was 280 nm. A standard curve of equation $y = 0.0156x - 0.026$ was obtained by using different concentrations of tetrahydrocurcumin (30, 40, 50, 60, and 70 $\mu\text{g/mL}$).

An indirect method was applied to calculate the entrapment efficiency of the Au-CuNPs, in which the supernatant obtained after centrifugation was used to determine the free amount of tetrahydrocurcumin. Next, the entrapment efficiency was calculated as the difference between the initial amount of tetrahydrocurcumin added and the free amount of tetrahydrocurcumin in the supernatant in regard to the total amount of tetrahydrocurcumin loaded in the Au-CuNP preparation (34).

Drug entrapment efficiency (DEE) was calculated from the formula: $DEE = (\text{Total drug conc.} - \text{Supernatant drug conc.}) / (\text{Total drug conc.}) \times 100 \%$. The loading capacity (LC %) was calculated from the following formula: $LC (\%) = (\text{Amount of total entrapped drug}) / (\text{Total nanoparticle weight}) \times 100 \%$.

Table 1. Zeta size distribution of 2 $\mu\text{g}/\mu\text{L}$ THC Au-CuNPs

| Record | Sample name | Z-average (d.nm) | PDI |
|------------|-------------|------------------|-------|
| 4 | THC-AuCuNPs | 251.4 | 0.231 |
| 5 | THC-AuCuNPs | 244 | 0.233 |
| 6 | THC-AuCuNPs | 251 | 0.219 |
| Mean value | | 248.8 | 0.228 |

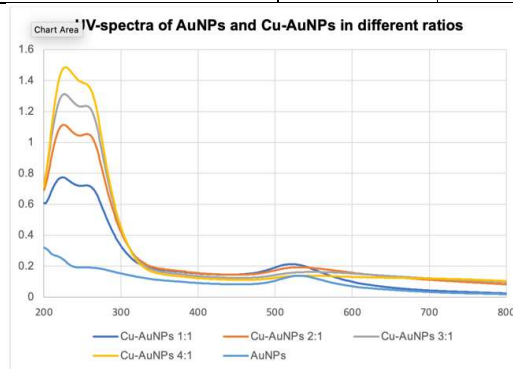


Figure 2: UV-spectra of AuNPs and Cu-AuNPs in different ratios

By scanning the colourless supernatant of THC Au-CuNPs under a UV spectrometer (Spectrum SP-UV 500DB, United Scientific, United States), the absorbance obtained at the tetrahydrocurcumin lambda max (280 nm) is shown in the table below (Table 1). By substituting the absorbance as shown in Table 1 into the equation $y = 0.0156x - 0.026$, the respective amount of drug remaining in each supernatant was obtained. Then, the entrapment efficiency of tetrahydrocurcumin in the Au-CuNPs was determined.

Example of calculation

By scanning the THC Au-CuNP supernatant with 0.5 mg of tetrahydrocurcumin, the absorbance of the supernatant was 0.8955. By inserting 0.8955 absorbance into the $y = 0.0156x - 0.026$ equation, the amount of drug entrapped was 59.07 $\mu\text{g}/\text{mL}$. Since the total volume of preparation was 10 mL, the total amount of drug in the supernatant was 590.7 μg . By subtracting the total amount of tetrahydrocurcumin remaining in the supernatant from the initial amount of tetrahydrocurcumin added, the amount of tetrahydrocurcumin entrapped in the Au-CuNPs was 90.7 μg .

When the concentration of tetrahydrocurcumin added increases, the drug uptake by nanoparticles increases. (35) Based on the calculation, 3 mg THC Au-CuNPs had the highest percentage of drug entrapment, 82.07 %. However, the particles in THC Au-CuNPs with 2.5 mg and 3 mg of tetrahydrocurcumin were too large, which could be seen by the naked eye. Therefore, 2 mg of tetrahydrocurcumin was selected as the amount of tetrahydrocurcumin added to prepare the THC Au-CuNP delivery system due to the highest possible amount of drug entrapment (54.17 %) with optimum nanoparticle size characteristics, in which the solution was clear and there was no aggregation of particles. From the calculation, there were 1083.4 μg of tetrahydrocurcumin entrapped in 500 μL of the preparation, and then 41 μL of ultrapure water was added to make the preparation have a concentration of 2 $\mu\text{g}/\mu\text{L}$ tetrahydrocurcumin in the THC Au-CuNP delivery system.

Zetasizer

The average of the readings was calculated after three cycles of measurement via dynamic light scattering (DLS) spectroscopy. The average peak provided the mean particle diameter of THC Au-CuNPs (36).

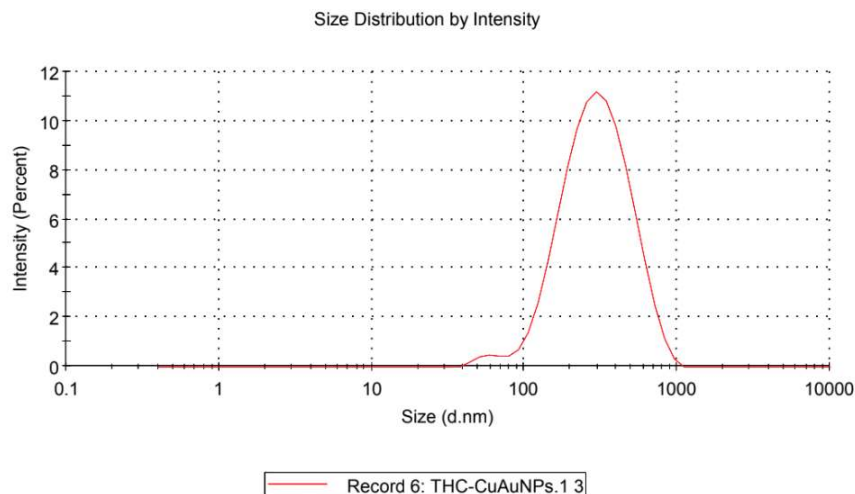


Figure 4: Zeta size distribution by intensity of 2 $\mu\text{g}/\mu\text{L}$ THC Au-CuNPs

Based on the results (table 1 and Figure 4), the mean particle diameter of 2 $\mu\text{g}/\mu\text{L}$ THC Au-CuNPs was 248.8 nm, indicating the successful formation of nanocomposites with a diameter of a few hundred nanometers (37). Nanoparticles are particles with a size range of subnanometer to a few hundred nanometers (37). A composite is composed of two or more different materials to merge their best characteristics. When one of the composite materials has one or more dimensions that are in the nano size range, the composite is known as a nanocomposite. (38) Particle size plays an important role in drug delivery to tumours (39,40). Studies have supported that the size range of endocytosed drug delivery systems within 100-1,000 nm will have increased bioavailability (41-43). Furthermore, nanoparticles smaller than 500 nm have improved cellular internalisation compared with nanoparticles larger than 500 nm (41,42). This is due to the larger surface area of nanoparticles, enabling extra ionic interactions with the biological membrane of the cells for endocytosis and phagocytosis to take place (41,44). Therefore, the mean particle diameter of 2 $\mu\text{g}/\mu\text{L}$ THC Au-CuNPs at 248.8 nm is desirable.

The polydispersity index (PDI), also termed the heterogeneity ratio, is a ratio of the molecular weight averages that is frequently used to describe the polymer molecular weight distribution and size distribution. (45, 46) The size distribution of particles is important in cellular internalisation, in which the formation of monodisperse nanoparticles is favoured (39). When the molecular weight distribution width increases, the polydispersity index increases (46). A PDI value of 0.0 indicates a homogeneous particle size of the sample, and a PDI value of 1.0 indicates a highly polydisperse particle size of the sample (39). The formation of AuNPs by the chemical reduction method usually has two major limitations. First, a very dilute AuNP solution is formed. Second, as the particle size increases, the size distribution widens, resulting in polydisperse AuNPs at sizes

exceeding 50 nm (33,45,47). Studies have shown that a smaller size and size distribution of AuNPs can be produced by reversing the order of the addition of citrate and gold (45,48,49). Based on the results (Table 1), the PDI obtained was 0.228, showing that the polydispersity of the preparation is acceptable. Reduction in polydispersity is associated with reduction in the diameter of the AuNPs produced (45, 50).

Dynamic monitoring of cytotoxic activity using the RTCA DP system

IC_{50} (half maximal inhibitory concentration) is the concentration of the drug required to inhibit biological or biochemical functions by half, which is used to estimate the effectiveness of the drug. Namely, drugs with larger IC_{50} values work less effectively than drugs with smaller IC_{50} values. (51,52) The IC_{50} value of tetrahydrocurcumin obtained following treatment of the Caco-2 cell line with tetrahydrocurcumin for 72 hours was 151.72 $\mu\text{g}/\text{mL}$, which indicated a moderate cytotoxic effect (53).

Three different amounts of THC Au-CuNPs (5 μL , 10 μL , and 15 μL), Au-CuNPs, and a negative control were tested for cell cytotoxicity. The cell number was standardised at 24 hours. From the results shown in Figure 5, the cytotoxicity of 10 μL and 15 μL THC Au-CuNPs was confirmed, as they successfully reduced the cell index to nearly zero, while 5

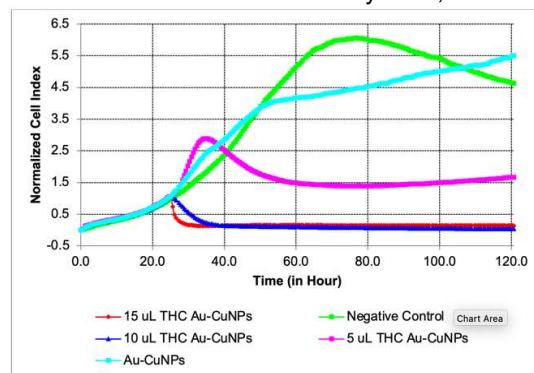


Figure 5. Cytotoxicity of THC Au-CuNPs on Caco-2 cells as demonstrated by the xCELLigence RTCA DP instrument.

μ L THC Au-CuNPs showed a slight reduction in the cell index. The concentration of THC Au-CuNPs prepared was 2 μ g/ μ L, so the amount of tetrahydrocurcumin in 5 μ L, 10 μ L, and 15 μ L of THC Au-CuNPs was 10 μ g, 20 μ g, and 30 μ g, respectively.

Conclusion

In this research, a Au-CuNP delivery system was successfully developed to carry tetrahydrocurcumin, named tetrahydrocurcumin gold-copper nanocomposites (THC Au-CuNPs). The preparation of the delivery system was based on the Turkevich method with citrate acting as a reducing agent and a capping agent. The delivery of tetrahydrocurcumin to colorectal cancer and its cytotoxic effect on colorectal cancer of tetrahydrocurcumin-loaded gold-copper nanocomposites (THC Au-CuNPs) were confirmed in this study. In the RTCA DP system-based dynamic monitoring of cytotoxic activity, the cytotoxicity of THC Au-CuNPs was confirmed at 10 μ g, 20 μ g, and 30 μ g, as they successfully reduced the cell index to nearly zero, and 30 μ g of THC Au-CuNPs reduced the cell index at the highest rate. Future studies could focus on further confirming the properties of the bioengineered delivery system of tetrahydrocurcumin through more characterisation studies and optimisation of the Au-CuNP delivery system to deliver tetrahydrocurcumin *in vivo*.

Acknowledgement

This project is supported by the Fundamental Research Grant Scheme (FRGS) (Reference code: FRGS/1/2021/SKK0/UCSI/02/5), Ministry of Higher Education (MOHE), and Research excellence and innovation grant (Project Code: REIG-FPS-2020-052) under the Centre of Excellence in Research, Value Innovation and Entrepreneurship (CERVIE), UCSI University, Malaysia.

Conflict of Interest

The authors declare no conflict of interest.

References

1. Bray F, Laversanne M, Weiderpass E, Soerjomataram I. The ever-increasing importance of cancer as a leading cause of premature death worldwide. *Cancer*. 2021;127(16):3029-30.
2. Sung H, Ferlay J, Siegel RL, Laversanne M, Soerjomataram I, Jemal A, et al. Global cancer statistics 2020: GLOBOCAN estimates of incidence and mortality worldwide for 36 cancers in 185 countries. *CA: a cancer journal for clinicians*. 2021;71(3):209-49.
3. Khatwani N, Adeyeni T, Ezekiel U. The Anti-Proliferative Effects of Curcumin Derivatives, Dimethoxycurcumin, Bisdemethoxycurcumin and Tetrahydrocurcumin, on DLD-1 Colon Cancer Cells. *The FASEB Journal*. 2016;30:1090.6-6.
4. Wu J-C, Tsai M-L, Lai C-S, Wang Y-J, Ho C-T, Pan M-H. Chemopreventative effects of tetrahydrocurcumin on human diseases. *Food & function*. 2013;5(1):12-7.
5. Kunnumakkara AB, Bordoloi D, Harsha C, Banik K, Gupta SC, Aggarwal BB. Curcumin mediates anticancer effects by modulating multiple cell signaling pathways. *Clinical science*. 2017;131(15):1781-99.
6. Irving GR, Howells LM, Sale S, Kralj-Hans I, Atkin WS, Clark SK, et al. Prolonged Biologically Active Colonic Tissue Levels of Curcumin Achieved After Oral Administration—A Clinical Pilot Study Including Assessment of Patient Acceptability Colonic Levels of Curcumin After Oral Administration—Clinical Study. *Cancer prevention research*. 2013;6(2):119-28.
7. FDA. FDA investigates two serious adverse events associated with ImprimisRx's compounded curcumin emulsion product for injection. 2017 [Available from:..
8. Kakkar V, Kaur IP, Kaur AP, Saini K, Singh KK. Topical delivery of tetrahydrocurcumin lipid nanoparticles effectively inhibits skin inflammation: *in vitro* and *in vivo* study. *Drug Development and Industrial Pharmacy*. 2018;44(10):1701-12.
9. Siviero A, Gallo E, Maggini V, Gori L, Mugelli A, Firenzuoli F, et al. Curcumin, a

- golden spice with a low bioavailability. *Journal of Herbal Medicine*. 2015;5(2):57-70.
10. Lai C-S, Ho C-T, Pan M-H. The cancer chemopreventive and therapeutic potential of tetrahydrocurcumin. *Biomolecules*. 2020;10(6):831.
 11. Plyduang T, Lomlim L, Yuenyongsawad S, Wiwattanapatapee R. Carboxymethyl cellulose-tetrahydrocurcumin conjugates for colon-specific delivery of a novel anticancer agent, 4-amino tetrahydrocurcumin. *European Journal of Pharmaceutics and Biopharmaceutics*. 2014;88(2):351-60.
 12. Mahal A, Wu P, Jiang ZH, Wei X. Schiff bases of tetrahydrocurcumin as potential anticancer agents. *Chemistry Select*. 2019;4(1):366-9.
 13. Chen S, Wu Q, Ma M, Huang Z, Vriesekoop F, Liang H. Designing biocompatible protein nanoparticles for improving the cellular uptake and antioxidation activity of tetrahydrocurcumin. *Journal of Drug Delivery Science and Technology*. 2021;63:102404.
 14. Holder GM, Plummer JL, Ryan AJ. The metabolism and excretion of curcumin (1, 7-bis-(4-hydroxy-3-methoxyphenyl)-1, 6-heptadiene-3, 5-dione) in the rat. *Xenobiotica*. 1978;8(12):761-8.
 15. Ravikumar R, Ganesh M, Senthil V, Ramesh YV, Jakki SL, Choi EY. Tetrahydrocurcumin loaded PCL-PEG electrospun transdermal nanofiber patch: Preparation, characterisation, and *in vitro* diffusion evaluations. *Journal of Drug Delivery Science and Technology*. 2018;44:342-8.
 16. Sugiyama Y, Kawakishi S, Osawa T. Involvement of the β -diketone moiety in the antioxidative mechanism of tetrahydrocurcumin. *Biochemical pharmacology*. 1996;52(4):519-25.
 17. Loron A, Gardrat C, Tabary N, Martel B, Coma V. Tetrahydrocurcumin encapsulation in cyclodextrins for water solubility improvement: Synthesis, characterisation and antifungal activity as a new biofungicide. *Carbohydrate Polymer Technologies and Applications*. 2021;2:100113.
 18. Ravindranath V, Chandrasekhara N. Absorption and tissue distribution of curcumin in rats. *Toxicology*. 1980;16(3):259-65.
 19. Pan K, Luo Y, Gan Y, Baek SJ, Zhong Q. pH-driven encapsulation of curcumin in self-assembled casein nanoparticles for enhanced dispersibility and bioactivity. *Soft Matter*. 2014;10(35):6820-30.
 20. Lagoa R, Silva J, Rodrigues JR, Bishayee A. Advances in phytochemical delivery systems for improved anticancer activity. *Biotechnology advances*. 2020;38:107382.
 21. Singh P, Pandit S, Mokkapatil V, Garg A, Ravikumar V, Mijakovic I. Gold Nanoparticles in Diagnostics and Therapeutics for Human Cancer. *Int J Mol Sci*. 2018;19(7).
 22. Amendola V, Pilot R, Frasconi M, Maragò OM, Iati MA. Surface plasmon resonance in gold nanoparticles: a review. *Journal of Physics: Condensed Matter*. 2017;29(20):203002.
 23. Ghosh P, Han G, De M, Kim CK, Rotello VM. Gold nanoparticles in delivery applications. *Advanced drug delivery reviews*. 2008;60(11):1307-15.
 24. Dang TMD, Le TTT, Fribourg-Blanc E, Dang MC. Synthesis and optical properties of copper nanoparticles prepared by a chemical reduction method. *Advances in Natural Sciences: Nanoscience and Nanotechnology*. 2011;2(1):015009.
 25. Biresaw SS, Taneja P. Copper nanoparticles green synthesis and characterisation as anticancer potential in breast cancer cells (MCF7) derived from *Prunus nepalensis* phytochemicals. *Materials Today: Proceedings*. 2022;49:3501-9.
 26. He R, Wang YC, Wang X, Wang Z, Liu G, Zhou W, et al. Facile synthesis of pentacle gold-copper alloy nanocrystals and their plasmonic and catalytic properties. *Nat Commun*. 2014;5:4327.
 27. Woźniak-Budych MJ, Langer K, Peplińska B, Przysięcka Ł, Jarek M, Jarzębski M, et al. Copper-gold nanoparticles:

- Fabrication, characteristic and application as drug carriers. *Materials Chemistry and Physics*. 2016;179:242-53.
28. Maki MAA, Kumar PV, Cheah S-C, Siew Wei Y, Al-Nema M, Bayazeid O, et al. Molecular Modelling-Based Delivery System Enhances Everolimus-Induced Apoptosis in Caco-2 Cells. *ACS Omega*. 2019;4(5):8767-77.
29. Faramarzi MA, Forootanfar H. Biosynthesis and characterisation of gold nanoparticles produced by laccase from *Paraconiothyrium variabile*. *Colloids and Surfaces B: Biointerfaces*. 2011;87(1):23-7.
30. Zhang YX, Wang YH. Nonlinear optical properties of metal nanoparticles: a review. *RSC advances*. 2017;7(71):45129-44.
31. Njoki PN, Lim IIS, Mott D, Park HY, Khan B, Mishra S, et al. Size Correlation of Optical and Spectroscopic Properties for Gold Nanoparticles. *The Journal of Physical Chemistry C*. 2007;111 (40):14664-9.
32. Manta P, Nagraik R, Sharma A, Kumar A, Verma P, Paswan SK, et al. Optical Density Optimisation of Malaria Pan Rapid Diagnostic Test Strips for Improved Test Zone Band Intensity. *Diagnostics*. 2020;10(11):880.
33. Kimling J, Maier M, Okenve B, Kotaidis V, Ballot H, Plech A. Turkevich method for gold nanoparticle synthesis revisited. *The Journal of Physical Chemistry B*. 2006;110(32):15700-7.
34. Gaikwad DV, Choudhari P, Bhatia N, Bhatia M. Characterisation of pharmaceutical nanocarriers: *in vitro* and *in vivo* studies. 2019. p. 33-58.
35. Busch W, Bastian S, Trahorsch U, Iwe M, Kühnel D, Meißner T, et al. Internalisation of engineered nanoparticles into mammalian cells *in vitro*: influence of cell type and particle properties. *Journal of Nanoparticle Research*. 2011;13(1):293-310.
36. Verma HN, Singh P, Chavan R. Gold nanoparticle: synthesis and characterisation. *Veterinary world*. 2014;7(2):72.
37. Huynh KH, Pham XH, Kim J, Lee SH, Chang H, Rho WY, et al. Synthesis, Properties, and Biological Applications of Metallic Alloy Nanoparticles. *Int J Mol Sci*. 2020;21(14).
38. Twardowski TE. Introduction to nanocomposite materials: properties, processing, characterisation: DEStech Publications, Inc; 2007.
39. Danaei M, Dehghankhold M, Ataei S, Hasanzadeh Davarani F, Javanmard R, Dokhani A, et al. Impact of Particle Size and Polydispersity Index on the Clinical Applications of Lipidic Nanocarrier Systems. *Pharmaceutics*. 2018;10(2).
40. Mozafari M, Pardakhty A, Azarmi S, Jazayeri J, Nokhodchi A, Omri A. Role of nanocarrier systems in cancer nanotherapy. *Journal of liposome research*. 2009;19(4): 310-21.
41. Murugan K, Choonara YE, Kumar P, Bijukumar D, du Toit LC, Pillay V. Parameters and characteristics governing cellular internalisation and trans-barrier trafficking of nanostructures. *Int J Nanomedicine*. 2015;10:2191-206.
42. Acosta E. Bioavailability of nanoparticles in nutrient and nutraceutical delivery. *Current opinion in colloid & interface science*. 2009;14(1):3-15.
43. Patel NR, Damann K, Leonardi C, Sabliov CM. Size dependency of PLGA-nanoparticle uptake and antifungal activity against *Aspergillus flavus*. *Nanomedicine*. 2011;6(8):1381-95.
44. Gratton SE, Ropp PA, Pohlhaus PD, Luft JC, Madden VJ, Napier ME, et al. The effect of particle design on cellular internalisation pathways. *Proceedings of the National Academy of Sciences*. 2008;105(33):11613-8.
45. Zabetakis K, Ghann WE, Kumar S, Daniel MC. Effect of high gold salt concentrations on the size and polydispersity of gold nanoparticles prepared by an extended Turkevich–Frens method. *Gold Bulletin*. 2012;45(4):203-11.

46. Rogošić M, Mencer HJ, Gomzi Z. Polydispersity index and molecular weight distributions of polymers. *European Polymer Journal*. 1996;32(11):1337-44.
47. Ji X, Song X, Li J, Bai Y, Yang W, Peng X. Size control of gold nanocrystals in citrate reduction: the third role of citrate. *J Am Chem Soc*. 2007;129(45):13939-48.
48. Ojea-Jiménez I, Bastús NG, Puntés V. Influence of the sequence of the reagents addition in the citrate-mediated synthesis of gold nanoparticles. *The Journal of Physical Chemistry C*. 2011;115(32):15752-7.
49. Sivaraman SK, Kumar S, Santhanam V. Monodisperse sub-10 nm gold nanoparticles by reversing the order of addition in Turkevich method--the role of chloroauric acid. *J Colloid Interface Sci*. 2011;361(2):543-7.
50. Li C, Li D, Wan G, Xu J, Hou W. Facile synthesis of concentrated gold nanoparticles with low size-distribution in water: temperature and pH controls. *Nanoscale Research Letters*. 2011;6(1):440.
51. W Caldwell G, Yan Z, Lang W, A Masucci J. The IC50 concept revisited. *Current topics in medicinal chemistry*. 2012; 12 (11):1282-90.
52. Neubig RR, Spedding M, Kenakin T, Christopoulos A. International Union of Pharmacology Committee on Receptor Nomenclature and Drug Classification. XXXVIII. Update on terms and symbols in quantitative pharmacology. *Pharmacological reviews*. 2003;55(4):597-606.
53. Indrayanto G, Putra GS, Suhud F. Chapter Six - Validation of *in vitro* bioassay methods: Application in herbal drug research. In: Al-Majed AA, editor. *Profiles of Drug Substances, Excipients and Related Methodology*. 46: Academic Press; 2021. p. 273-307.